Received: 4 October 2022 | Accepted: 9 February 2023

DOI: 10.1111/aos.15650

Acta Ophthalmologica

ORIGINAL ARTICLE

Diagnostic accuracy of retinal optical coherence tomography in children with a newly diagnosed brain tumour

Myrthe A. Nuijts[1] | **Inge Stegeman**[1,2,3] | **Giorgio L. Porro**[1] | **Carlien A. M. Bennebroek**[4] | **Tom van Seeters**[5] | **Frank A. Proudlock**[6] | **Antoinette Y. N. Schouten – van Meeteren**[7] | **Saskia M. Imhof**[1]

[1]Department of Ophthalmology, University Medical Centre Utrecht, Utrecht, The Netherlands

[2]Department of Otorhinolaryngology and Head & Neck Surgery University, University Medical Centre Utrecht, Utrecht, The Netherlands

[3]Brain Centre, University Medical Centre Utrecht, Utrecht, The Netherlands

[4]Department of Ophthalmology, Amsterdam UMC, Location University of Amsterdam, Amsterdam, The Netherlands

[5]Department of Radiology, Elisabeth-TweeSteden Hospital, Tilburg, The Netherlands

[6]University of Leicester Ulverscroft Eye Unit, Leicester, UK

[7]Department of Neuro-Oncology, Princess Máxima Centre for Paediatric Oncology, Utrecht, The Netherlands

Correspondence
Myrthe A. Nuijts, Department of Ophthalmology, University Medical Centre Utrecht, PO Box 85500, 3508 GA, Utrecht, The Netherlands.
Email: m.a.nuijts@umcutrecht.nl

Funding information
Stichting Kinderen Kankervrij, Grant/Award Number: 304

Abstract

Purpose: To estimate the diagnostic accuracy of circumpapillary retinal nerve fibre layer (RNFL) thickness and macular ganglion cell layer–inner plexiform layer (GCL-IPL) thickness measurements to discriminate an abnormal visual function (i.e. abnormal age-based visual acuity and/or visual field defect) in children with a newly diagnosed brain tumour.

Methods: This cross-sectional analysis of a prospective longitudinal nationwide cohort study was conducted at four hospitals in the Netherlands, including the national referral centre for paediatric oncology. Patients aged 0–18 years with a newly diagnosed brain tumour and reliable visual acuity and/or visual field examination and optical coherence tomography were included. Diagnostic accuracy was evaluated with sensitivity, specificity, positive predictive value (PPV) and negative predictive value (NPV).

Results: Of 115 patients included in the study (67 [58.3%] male; median age 10.6 years [range, 0.2–17.8 years]), reliable RNFL thickness and GCL-IPL thickness measurements were available in 92 patients (80.0%) and 84 patients (73.0%), respectively. The sensitivity for detecting an abnormal visual function was 74.5% for average RNFL thickness and 41.7% for average GCL-IPL thickness at a specificity of 44.5% and 82.9%, respectively. The PPV and NPV were 33.0% and 82.6% for the average RNFL thickness and 57.1% and 82.2% for the average GCL-IPL thickness.

Conclusion: An abnormal visual function was discriminated correctly by using the average RNFL thickness in seven out of ten patients and by using the average GCL-IPL thickness in four out of ten patients. The relatively high NPVs signified that patients with normal average RNFL thickness and average GCL-IPL thickness measurements had a relative high certainty of a normal visual function.

KEYWORDS
adolescent, brain tumour, child, optical coherence tomography, visual acuity, visual field, visual function

1 | INTRODUCTION

Visual sequelae are a common adverse effect in childhood brain tumour survivors (Armstrong, 2010; Armstrong et al., 2011; Vinchon et al., 2011). The prevalence of visual sequelae reported in the literature ranges between 15% and 67% and depends on the subtype and location of the brain tumour, the presence of increased intracranial pressure and the given treatment modality (Armstrong et al., 2011; Pillai et al., 2012; Saha et al., 2014; Vinchon et al., 2011).

Ophthalmological surveillance at diagnosis and during follow-up in children with a brain tumour is of great importance for early detection of vision loss and

Antoinette Y. N. Schouten – van Meeteren and Saskia M. Imhof contributed equally to this work.

Myrthe A. Nuijts is a member of the Dutch Ophthalmological Societies.

to provide treatment to potentially preserve visual function. In particular, in children with an optic pathway glioma (OPG), treatment is often only initiated once new or progressive vision loss has been identified. However, accurate measurement of visual function (i.e. visual acuity [VA] and visual field [VF]) can be challenging in children with a brain tumour. Impaired neurologic status, fatigue and young age are issues that can limit cooperation and thereby reduce the reliability of standard ophthalmological testing methods (Avery et al., 2013). The inability to reliably assess the visual function puts these children at increased risk to develop significant and permanent vision loss before treatment has been initiated. Therefore, a reliable non-behavioural ophthalmological testing method, independent of a child's cooperation, might provide more objective opportunities to estimate the visual function in all children with a newly diagnosed brain tumour.

A promising non-behavioural objective testing method for ophthalmological surveillance is spectral-domain optical coherence tomography (OCT). OCT is a non-invasive imaging modality that applies low-coherence interferometry to measure the thickness of separate retinal layers (Avery, Rajjoub, et al., 2015; Fercher, 2010). A spectral-domain handheld OCT device could be used to image the retinal layers in young and/or non-cooperative children with a variety of conditions (Avery et al., 2014; Gu et al., 2014). In the past decade, several investigators have described that a decrease in visual function (i.e. decreased VA and VF defects) is associated with thinning of the circumpapillary retinal nerve fibre layer (RNFL) and macular ganglion cell layer – inner plexiform layer (GCL-IPL) in children with an OPG (Avery et al., 2014; Avery, Cnaan, et al., 2015; Fard et al., 2013; Gu et al., 2014; Parrozzani et al., 2018). In a recent systematic review, we found that studies evaluating the diagnostic accuracy of circumpapillary RNFL thickness and macular GCL-IPL thickness measurements for estimating the visual function (VA and VF) in different subtypes of brain tumours in children are lacking (Nuijts, Imhof, et al., 2021). Therefore, we aimed to prospectively investigate the diagnostic accuracy of circumpapillary RNFL thickness and macular GCL-IPL thickness measurements to discriminate an abnormal visual function in children recently diagnosed with a brain tumour.

2 | METHODS

2.1 | Study design and patients

For this cross-sectional study, data was obtained from a prospective longitudinal nationwide cohort study investigating visual impairment in children newly diagnosed with a brain tumour in the Netherlands (Dutch Trial Register, identifier: NL7697; Nuijts et al., 2019). The study was conducted in compliance with the Helsinki principles and was approved by the Medical Ethical Committee Utrecht as part of the CCISS study (identifier: 19-106/M). After full explanation of the nature of the study, written informed consent was obtained from all parents or legal guardian(s) of children <16 years of age and from children aged 12–18 years. Consecutive children, aged 0–18 years, with a newly diagnosed brain tumour between 15 May 2019, and 11 August 2021, were eligible for inclusion in this study. Inclusion of children and the ophthalmological examination took place at the Princess Máxima Centre for Paediatric Oncology Utrecht, University Medical Centre Utrecht, Amsterdam University Medical Centre and Erasmus Medical Centre Rotterdam. In some children the ophthalmological examination took place at the University Medical Centre Groningen prior to proton therapy. All children underwent a comprehensive ophthalmological examination including orthoptic examination, VA, fundus examination, VF examination and OCT within 4 weeks from brain tumour diagnosis. Children without reliable OCT and/or VA or VF examination at diagnosis were excluded in this cross-sectional study. Data were captured using electronic case report forms.

2.2 | Clinical and radiological characteristics

Clinical characteristics were collected from electronic health records using a standardized format that included age at brain tumour diagnosis, sex, medical history (including diagnosis of neurofibromatosis type 1) and tumour histology. Histopathological data were obtained from the original pathology reports and included tumour staging according to the World Health Organization classification (Louis et al., 2016). Diagnostic MRIs were assessed independently by two medical reviewers, blinded to the patient's clinical status, to obtain the location of the brain tumour, the presence and degree of hydrocephalus and involvement of the optic pathway. Discrepancies between reviewers were discussed with an experienced neuro-radiologist. The presence and extent of hydrocephalus was described following the classification of Traunwieser et al. and was restricted to three grades: minor hydrocephalus (enlarged ventricles only), moderate hydrocephalus (enlarged ventricles and additional periventricular fluid accumulation) and severe hydrocephalus (enlarged ventricles, periventricular fluid accumulation and additional flattened cerebral sulci at the vertex; Traunwieser et al., 2020). Based on the location, brain tumours were classified into three groups: supratentorial cerebral hemisphere tumours, supratentorial midline tumours and infratentorial tumours. Two particular types of supratentorial midline tumours in which the optic pathway is often involved have been analysed in more detail, namely OPGs and craniopharyngiomas. Involvement of the optic pathway by OPGs was classified according to the modified Dodge classification. The most posterior tumour location was assigned to OPGs involving multiple regions (Taylor et al., 2008).

2.3 | OCT image acquisition, analysis and definitions

Quantitative circumpapillary RNFL thickness and macular GCL-IPL thickness measurements serve as index tests and were obtained within 4 weeks from diagnosis

using either a tabletop OCT (Cirrus HD OCT 5000, Zeiss Meditec AG, Germany or Spectralis SD-OCT, Heidelberg Engineering) or handheld OCT (Bioptigen). Clinical information and reference standard results were not available to the assessors of the index tests.

In children old enough to cooperate and who were evaluated at the University Medical Centre Utrecht, circumpapillary RNFL thickness and macular GCL-IPL thickness measurements were acquired with the tabletop Carl Zeiss Cirrus HD OCT 5000 (Carl Zeiss Meditec AG). Circumpapillary RNFL measurements including average and quadrant-specific (i.e. superior, nasal, inferior and temporal) thicknesses were automatically calculated using the Optic Disc Cube 200×200 protocol. Macular GCL-IPL measurements including average, minimum and sector-specific (i.e. average, minimum, supero-temporal, superior, supero-nasal, infero-nasal, inferior and infero-temporal) thicknesses were automatically calculated using the Macular Cube 200×200 protocol. Scans with a signal strength <6 dB were discarded. In children who were evaluated at the Amsterdam University Medical Centre or Erasmus Medical Centre Rotterdam, circumpapillary RNFL thickness measurements were acquired with the tabletop Spectralis SD-OCT (Heidelberg Engineering GmbH) in high-speed mode using the eye tracking feature to accurately centre, a 3.5 mm circle over the optic nerve head. Average and quadrant-specific (i.e. superior, nasal, inferior and temporal) RNFL thicknesses were automatically recorded. Scans with a signal strength <20 dB were discarded. The Spectralis SD-OCT device used in this study does not segment the GCL-IPL, and therefore, GCL-IPL thickness measurements were not available for children evaluated with the Spectralis SD-OCT. All OCT scans were reviewed for centration or segmentation errors and image artefacts by two examiners (M.A.N., S.M.I.). Scans with segmentation errors and/or unreliable thickness measurements due to papilledema were excluded. RNFL thickness and GCL-IPL thickness measurements were considered abnormal when they fall outside the age-based 95% confidence interval (CI) for RNFL thickness or GCL-IPL thickness for the particular OCT device (Barrio-Barrio et al., 2013; Pérez-García et al., 2015).

In young children who were not able to cooperate with tabletop OCT imaging and who were evaluated at the University Medical Centre Utrecht, handheld OCT imaging (Bioptigen) was performed during sedation after children had undergone MRI as part of their routine clinical care. Children received mydriatic eye drops (0.5% tropicamide and 2.5% phenylephrine hydrochloride) before undergoing MRI. The handheld OCT was performed during slight prolongation of continuous infusion of propofol to maintain adequate sedation. The examiner was positioned at the head of the bed, and eyelids were moved away from the pupil by the examiner's fingers. The handheld OCT lens was held between the index finger and thumb and was placed over the patient's eye. Movement of the handheld OCT probe was minimized by placing the other fingers against the forehead of the patient. According to previous recommendations, the working distance between the handheld OCT probe and the cornea was adjusted based on the child's axial length (Maldonado et al., 2010). Volumetric OCT images were acquired using a 10 mm×10 mm horizontal raster scan protocol (600 A-scans×80 B-scan). According to a previous study protocol (Shah et al., 2020), images were converted using an ImageJ script into a format that could be imported into Copernicus SR Analysis software (Optopol Technology). Circumpapillary RNFL thickness measurements including average and quadrant-specific (i.e. superior, nasal, inferior and temporal) thicknesses were assessed at 6° radii from the optic disc centre. The computer software algorithm used for the automatic segmentation of the handheld OCT scans does not calculate the GCL-IPL thickness, and therefore, these measurements were not available in children imaged with the handheld OCT. The handheld OCT delivers information on the continuous RNFL thickness measurements. Scans with segmentation errors and/or unreliable thickness measurements due to papilledema were excluded. Age-based 95% CIs are not yet available for this particular OCT device, so diagnostic accuracy could not be calculated.

2.4 | VA and VF outcomes and definitions

All children underwent a VA and/or VF examination within 4 weeks from brain tumour diagnosis, which serve as reference standard for the visual function. Clinical information (i.e. tumour type and location) and index test results were partial available to the assessors of the reference standard. Best-corrected visual acuity (BCVA) was measured for each eye separately (monocular VA) using age-appropriate tests (e.g. Teller Acuity Cards, Cardiff Acuity Test, Kay Pictures, E-charts, numeral or Snellen Chart). Binocular VA was measured when monocular VA measurement failed. BCVA was converted to the logarithm of the minimum angle of resolution (logMAR) for statistical purposes. The VF was measured by using age-appropriate tests including the Behavioural Visual Field (BEFIE) Screening test (Koenraads et al., 2015), the semiautomatic static Peritest (Greve et al., 1982), Goldmann kinetic perimetry (Quinn et al., 1991) or the Humphrey Visual Field Analyser (HFA; SITA 24-2 FAST algorithm; Donahue & Porter, 2001). Assessment of the VF was performed blinded by two individual graders (G.L.P. and M.A.N.) to avoid misclassification. Both the presence and type of VF defects were scored according to predefined definitions. Results of the BEFIE test were categorized as normal when the peripheral visual field (PVF) extended ≥40° nasally and ≥70° temporally, or according to age-specific PVF limits in patients under 5 years of age. PVF defects were further classified into symmetric (concentric) and asymmetric or homonymous defects (Koenraads et al., 2015). Results of the HFA 24-2 SITA-FAST or semiautomatic-static Peritest were defined as abnormal when three or more contiguous points reached significance ($p < 0.05$). Results of Goldmann perimetry were classified as abnormal when there was a constriction greater than 10° across a minimum of three contiguous 15° vectors. Humphrey 24-2 SITA-FAST tests were excluded when false-positive errors, false negative errors and fixation losses were greater or equal to 20% (Avery, Cnaan, et al., 2015; Biousse & Newman, 2015).

Discrepancies between graders were resolved by discussion between them. Patients with unreliable VA and VF measurements were excluded from further analysis. An abnormal visual function was defined as VA ≥0.2 logMAR below normal age-based norms and/or a VF defect.

2.5 | Outcome measures and statistical analysis

All patients with reliable VA and/or VF examination and OCT were included in the analysis. Baseline characteristics and continuous circumpapillary RNFL thickness and macular GCL-IPL thickness measurements (microns) obtained both by tabletop OCT and handheld OCT were summarized using standard descriptive statistics (e.g. median and range for non-parametric distributed variables and number and percentage for categorical variables).

A patient was considered screen positive if there was an abnormal visual function (i.e. abnormal age-based VA measurement and/or VF defect) at the specified age-based cut-off level for the two index tests (i.e. circumpapillary RNFL thickness [average, superior, nasal, inferior or temporal thickness] and macular GCL-IPL thickness [average, minimum, supero-temporal, superior, supero-nasal, infero-nasal, inferior and infero-temporal thickness]). Diagnostic accuracy for the tabletop OCT devices is reported as sensitivity (proportion of patients with a true positive index test result [i.e. abnormal RNFL thickness or GCL-ILP thickness measurement] that have an abnormal visual function [i.e. abnormal age-based VA and/or VF defect]), specificity (proportion of patients with a true negative index test result [i.e. normal RNFL or GCL-ILP thickness measurement] that have a normal visual function [i.e. normal age-based VA and VF examination]), positive predictive value (PPV; proportion of patients with a true positive index test result divided by the group of patients with a true positive and false-positive index test result) and negative predictive value (NPV) (proportion of patients with a true negative index test result divided by the group of patients with a true negative and false negative index test result). Diagnostic accuracy was estimated for the total group of patients and for particular tumour subgroups in which the optic pathway is involved (i.e. OPGs and craniopharyngiomas). Results were reported according to the standards for reporting of diagnostic accuracy (Bossuyt et al., 2003). The collected data were analysed using STATISTICAL PACKAGE FOR THE SOCIAL SCIENCES (version 26.0.0.1, SPSS Inc.).

3 | RESULTS

3.1 | Patient population

A total of 230 eyes of 115 patients with a newly diagnosed brain tumour were included (Figures 1 and 2). Fifty-five of the initial 170 patients [32.4%] of our CCISS cohort were excluded because OCT imaging was not performed at diagnosis (N = 42 [24.6%]; logistical reasons [N = 32, 18.8%], inability of the patient to cooperate with testing [N = 6, 3.5%] or poor clinical condition of the patient [N = 4, 2.4%]), OCT imaging was unreliable (N = 8 [4.7%]) or no reference standard (i.e. VA or VF examination) was performed at diagnosis (N = 5 [2.9%]).

Table 1 provides an overview of the baseline characteristics. The median age was 10.6 years (range, 0.2–17.8 years), 67 of 115 (58.3%) were male. The tumour was located infratentorial in 58 (50.4%) patients, in the supratentorial midline in 33 (28.7%) patients and in the cerebral hemispheres in 24 (20.9%) patients. Nine (27.3%) and 11 (33.3%) patients with a supratentorial midline tumour were diagnosed with an OPG (bilateral, N = 6 [66.7%]; unilateral, N = 3 [33.3%]) and 11 (33.3%) and craniopharyngioma, respectively.

3.2 | Results of VA testing and VF examination

Both VA and VF examination were performed in 91 of all 115 included patients (79.1%); in 24 of 115 patients (20.9%) only VA examination was performed. Of the total of 115 patients, 52 eyes of 31 patients (27.0%) had an abnormal visual function (i.e. abnormal age-based VA and/or VF defect). Twelve eyes of 10 patients (8.7%) presented with an abnormal age-based VA only, 27 eyes of 18 patients (15.7%) with a VF defect only and 13 eyes of nine patients (7.8%) with both an abnormal age-based VA and VF defect.

3.3 | Characteristics of tabletop circumpapillary RNFL thickness measurements

In total, tabletop circumpapillary RNFL thickness measurements were available for 175 eyes of 92 patients (Figure 1). Fifty-five of 230 eyes (23.9%) of the baseline cohort had to be excluded from RNFL thickness measurements analyses as RNFL thickness measurements were performed with the handheld OCT device (N = 32 [13.9%]), were not performed (N = 14 [6.1%]) or were unreliable (N = 9 [3.9%]). Table 2 demonstrates the results of the continuous tabletop circumpapillary RNFL thickness measurements (i.e. average, superior, nasal, inferior and temporal thickness) for eyes with a normal visual function (N = 128 eyes [73.1%]; median average circumpapillary RNFL thickness, 105 µm [range, 82–329 µm]) and eyes with an abnormal visual function (N = 47 eyes [26.9%]; median average circumpapillary RNFL thickness, 204 µm [range, 59–605 µm]). For the subgroup of children with an OPG (N = 13 eyes [7.4%]), eyes with a normal visual (N = 8 eyes [61.5%]) function showed greater average circumpapillary RNFL thickness (median, 105 µm [range, 82–329 µm]) compared to eyes with an abnormal visual function (N = 5 eyes [38.5%]; median, 82 µm [range, 59–145 µm]). In the subgroup of children with craniopharyngioma (N = 22 eyes [12.6%]), the average circumpapillary RNFL thickness was lower in eyes with a normal visual function (N = 12 eyes [54.5%]; median, 104 µm [range, 88–258 µm]) compared to eyes with an abnormal visual function (N = 10 eyes [45.5%]; median, 111 µm [range, 83–282 µm]).

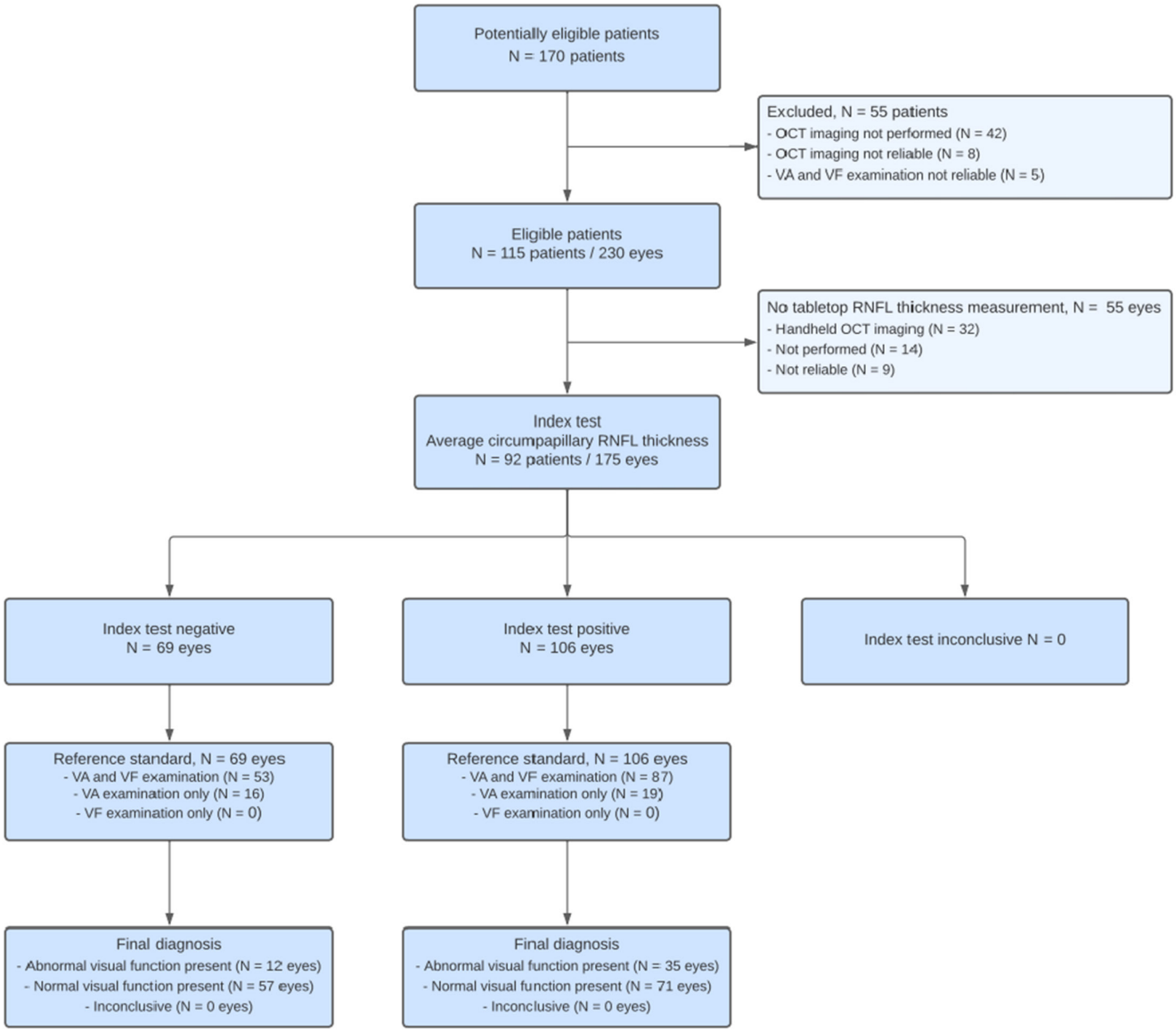

FIGURE 1 Study flow for average circumpapillary retinal nerve fibre layer thickness measurements. Flow-chart according to standards for reporting diagnostic accuracy. OCT, optical coherence tomography; RNFL, retinal nerve fibre layer; VA, visual acuity; VF, visual field.

3.4 | Characteristics of handheld circumpapillary RNFL thickness measurements

In total, 26 eyes of 16 patients were available for handheld circumpapillary RNFL thickness measurements at brain tumour diagnosis (i.e. average, superior, nasal, inferior and temporal thickness; Table 2). Six of 32 eyes (18.8%) of the total cohort of handheld circumpapillary RNFL OCT measurements were excluded due to unreliable measurements due to severe papilledema (N = 3 [50.0%]) or insufficient image quality (N = 3 [50.0%]). The median average circumpapillary RNFL thickness was 117 µm (range, 86–209 µm). Subgroup analyses were not performed due to a small sample size.

3.5 | Diagnostic accuracy of tabletop circumpapillary RNFL thickness measurements

The diagnostic accuracy of tabletop circumpapillary RNFL thickness measurements (i.e. average, superior, nasal, inferior and temporal thickness) in detecting an abnormal visual function at the age-based cut-off levels is summarized in Table 3. In the total group of eyes (N = 175), 35 of 47 eyes (74.5%) with an abnormal visual function had an abnormal average circumpapillary RNFL thickness measurement (true positives). Fifty-seven of 128 eyes (44.5%) had a normal visual function and a normal average circumpapillary RNFL thickness measurement (true negatives). Therefore, the average circumpapillary RNFL thickness had a sensitivity of 74.5% at a specificity of 44.5%. The PPV and NPV of the average circumpapillary RNFL thickness for an abnormal visual function are 33.0% and 82.6%, respectively. For the subgroup of patients with an OPG (N = 13 eyes [7.4%]), four of five eyes (80.0%) with an abnormal visual function had an abnormal average circumpapillary RNFL thickness measurement. Six of eight eyes (75.0%) had a normal visual function and a normal average circumpapillary RNFL thickness measurement. Corresponding numbers for the sensitivity, specificity, PPV and NPV were 80.0%, 75.0%, 66.7% and 85.7%,

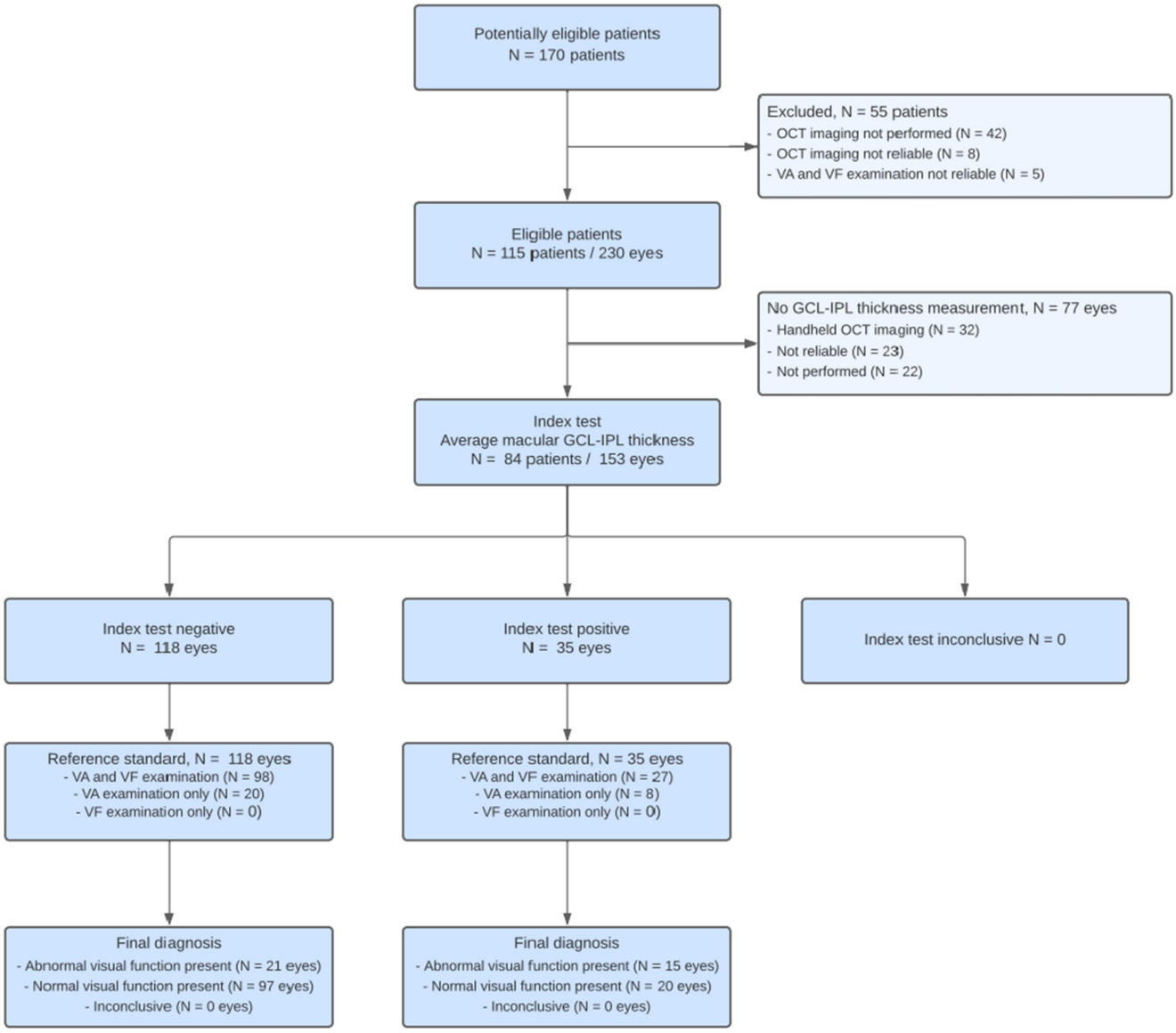

FIGURE 2 Study flow for average macular ganglion cell layer – inner plexiform layer thickness measurements. Flow-chart according to standards for reporting diagnostic accuracy. GCL-IPL, ganglion cell layer – inner plexiform layer; OCT, optical coherence tomography; RNFL, retinal nerve fibre layer; VA, visual acuity; VF, visual field.

respectively (Table S1). For the subgroup of patients with craniopharyngioma ($N = 22$ eyes [12.6%]), four of 10 eyes (40.0%) with an abnormal visual function had an abnormal average circumpapillary RNFL thickness measurement. Nine of 12 eyes (75.0%) had a normal visual function and a normal average circumpapillary RNFL thickness measurement. Sensitivity, specificity, PPV and NPV for average circumpapillary RNFL thickness measurement in this patient group were 40.0%, 75.0%, 57.1% and 60.0%, respectively (Table S2).

3.6 | Characteristics of macular GCL-IPL thickness measurements

In total, GCL-IPL thickness measurements were available for 153 eyes of 84 patients (Figure 2). Seventy-seven eyes (33.5%) of the baseline cohort were excluded from GCL-IPL thickness measurements analyses because handheld OCT was performed ($N = 32$ [13.9%]), GCL-IPL thickness measurements were unreliable ($N = 23$ [10%]) or not performed ($N = 22$ [9.6%]). Table 4 shows the results of the continuous GCL-IPL thickness measurements (i.e. average, minimum, supero-temporal, superior, supero-nasal, infero-nasal, inferior and infero-temporal thickness) for eyes with a normal visual function ($N = 117$ eyes [76.5%]; median average macular GCL-IPL thickness, 84 µm [range, 57–100 µm]) and eyes with an abnormal visual function ($N = 36$ eyes [23.5%]; median average macular GCL-IPL thickness, 78 µm [range, 54–94 µm]). For the subgroup of children with an OPG ($N = 15$ eyes), eyes with a normal visual function showed greater average macular GCL-IPL thickness (median, 76 µm [range, 61–87 µm]) compared to eyes with an abnormal visual function (median, 62 µm [range, 54–71 µm]). Also, in children with a craniopharyngioma the average macular GCL-IPL thickness was greater in eyes with a normal visual function (median, 85 µm [range, 57–96 µm]) compared to eyes with an abnormal visual function (median, 72 µm [range, 64–80 µm]).

TABLE 1 Baseline patient characteristics.

Characteristic	Total ($N = 115$)
Age at diagnosis, years	
Median [range]	10.6 [0.2–17.8]
0–5	24 (20.9)
>5–10	30 (26.1)
>10–15	42 (36.5)
>15	19 (16.5)
Male sex	67 (58.3)
Neurofibromatosis type 1[a]	4 (3.5)
Tumour histology	
Low-grade glioma	54 (47.0)
High-grade glioma	15 (13.0)
Medulloblastoma	8 (7.0)
Craniopharyngioma	8 (7.0)
Ependymoma	6 (5.2)
Germ cell tumour	7 (6.1)
Other[b]	8 (7.0)
Without histology[c]	9 (7.5)
Tumour location	
Supratentorial	57 (49.6)
Cerebral hemispheres	24 (20.9)
Midline	33 (28.7)
Thalamus	5
Pituitary gland	11
Optic pathways and/or optic chiasm	9
Pineal gland[d]	8
Infratentorial	58 (50.4)
Optic pathway involvement by optic pathway gliomas	9 (7.8)
Modified Dodge classification[e]	
1a. Single optic nerve	0
1b. Bilateral optic nerve	0
1c. Cisternal segment optic nerve	2 (1.7)
2a. Central chiasmatic	1 (0.9)
2b. Asymmetric chiasmatic	1 (0.9)
3. Optic tracts	1 (0.9)
3b. Asymmetric tracts	4 (3.5)
4. Diffuse posterior tracts	0
4b. Asymmetric posterior tracts	0
Hydrocephalus at diagnosis[f]	
None	32 (27.8)
Minor	12 (10.4)
Moderate	52 (45.2)
Severe	15 (13.0)
No information	4 (3.5)

Note: Data are presented as *N* (%) or as median [range].

[a]Diagnosis of neurofibromatosis type I is based on genetic testing.

[b]Atypical teratoid rhabdoid tumour ($N = 2$); meningioma ($N = 1$); pineoblastoma ($N = 1$); plexus tumour ($N = 2$); dysembryoplastic neuroepithelial tumour ($N = 1$); hemangioblastoma ($N = 1$).

[c]Radiological suspicion of optic pathway glioma ($N = 3$); radiological suspicion of non-optic pathway low-grade glioma ($N = 1$); serum/cerebrospinal fluid markers of germ cell tumour ($N = 5$).

[d]Two patients with bifocal germinoma localized in the pineal gland and pituitary gland were classified as having pineal region tumour.

[e]Optic pathway gliomas were classified according to the modified Dodge classification of Taylor et al., Br J Radiol, 2008. The most posterior tumour location was assigned to OPGs involving multiple regions.

[f]Hydrocephalus was classified according to the classification of Traunwieser et al., Neuro-Oncology Adv, 2020.

3.7 | Diagnostic accuracy of macular GCL-IPL thickness measurements

The diagnostic accuracy of macular GCL-IPL thickness measurements (i.e. average, minimum, supero-temporal, superior, supero-nasal, infero-nasal, inferior and infero-temporal thickness) in detecting an abnormal visual function at the age-based cut-off levels is summarized in Table 5. In the total group of eyes ($N = 153$), 15 of 36 eyes (41.7%) with an abnormal visual function had an abnormal average macular GCL-IPL thickness measurement (true positives). Ninety-seven of 117 eyes (82.9%) had a normal visual function and a normal average macular GCL-IPL thickness measurement (true negatives). Therefore, the average macular GCL-IPL thickness had a sensitivity of 41.7% at a specificity of 82.9%. The PPV and NPV of the average macular GCL-IPL thickness for an abnormal visual function are 57.1% and 82.2%, respectively. For the subgroup of patients with an OPG ($N = 15$ eyes [9.8%]), six of six eyes (100.0%) with an abnormal visual function had an abnormal average macular GCL-IPL thickness measurement. Five of nine eyes (55.6%) had a normal visual function and a normal average macular GCL-IPL thickness measurement. Corresponding numbers for the sensitivity, specificity, PPV and NPV were 100.0%, 55.6%, 60.0% and 100.0%, respectively (Table S3). For the subgroup of patients with craniopharyngioma ($N = 25$ eyes [16.3%]), seven of 10 eyes (70.0%) with an abnormal visual function had an abnormal average macular GCL-IPL thickness measurement. Twelve of 15 eyes (80.0%) had a normal visual function and a normal average macular GCL-IPL thickness measurement. Sensitivity, specificity, PPV and NPV for average macular GCL-IPL thickness measurement in this patient group were 70.0%, 80.0%, 70.0% and 80.0%, respectively (Table S4).

4 | DISCUSSION

In this prospective nationwide study in the Netherlands, we investigated the diagnostic accuracy of circumpapillary RNFL thickness and macular GCL-IPL thickness measurements to discriminate an abnormal visual function (i.e. abnormal age-based VA and/or VF defect) in children with a newly diagnosed brain tumour.

The NPVs of the average circumpapillary RNFL thickness (82.6%) and average macular GCL-IPL thickness (82.2%) are relatively high, but the PPVs (respectively 33.0% and 57.1%) are low, showing that the diagnostic capacity of circumpapillary RNFL thickness and macular GCL-IPL thickness measurements is moderate, which is in line with the low to moderate sensitivity and specificity of the thickness measurements. Our findings show that seven to eight out of 10 children with an abnormal visual function are discriminated correctly by the average circumpapillary RNFL thickness and four out of 10 children with an abnormal visual function are discriminated correctly by the average macular GCLP-IPL thickness. This while four out of 10 children and eight out of 10 with a normal visual function are detected as such with the average circumpapillary RNFL thickness and the average macular GCL-IPL thickness, respectively.

TABLE 2 Characteristics of circumpapillary retinal nerve fibre layer thickness measurements in children with a normal and abnormal visual function.

		Normal visual function			Abnormal visual function		
	Total	Total	OPG	Craniopharyngioma	Total	OPG	Craniopharyngioma
Tabletop OCT	**(*N* = 175)**	**(*N* = 128)**	**(*N* = 8)**	**(*N* = 12)**	**(*N* = 47)**	**(*N* = 5)**	**(*N* = 10)**
RNFL thickness, median (range), μm							
Average	123.5 (59–605)	118 (77–498)	105 (82–329)	104 (88–258)	204 (59–605)	82 (59–145)	110.5 (83–282)
Superior	163.5 (81–693)	152 (83–639)	144.5 (103–377)	131 (107–352)	264 (81–693)	106 (81–212)	131 (107–347)
Nasal	98.5 (49–545)	91 (49–514)	68.5 (56–323)	78 (58–180)	156 (51–545)	72 (51–86)	99 (56–350)
Inferior	159.0 (48–815)	152 (77–680)	131.5 (108–429)	124 (106–380)	245 (48–815)	114 (48–198)	157 (105–344)
Temporal	81.5 (37–608)[a]	78 (42–442)[a]	69.5 (44–190)	76 (61–121)[a]	94 (37–608)	57 (37–83)	48 (41–94)
Handheld OCT	**(*n* = 26)**	**(*n* = 25)**	**(*n* = 1)**	**(*n* = 0)**	**(*n* = 1)**	**(*n* = 0)**	**(*n* = 0)**
RNFL thickness, median (range), μm							
Average	117 (86–209)	116 (86–209)	130	NA	187	NA	NA
Superior	130 (101–280)	128 (101–280)	132	NA	185	NA	NA
Nasal	95.5 (85–232)	95 (58–232)	114	NA	185	NA	NA
Inferior	136 (83–227)	133 (83–227)	171	NA	226	NA	NA
Temporal	71.5 (50–100)	71 (50–97)	51	NA	100	NA	NA

Note: Data are presented as median (range).

Abbreviations: OCT, optical coherence tomography; OPG, optic pathway glioma; RNFL, retinal nerve fibre layer.

[a]Measurement of the temporal retinal nerve fibre layer thickness is missing for one eye.

TABLE 3 Diagnostic accuracy of tabletop circumpapillary retinal nerve fibre layer thickness.

Location	Abnormal visual function (*n*/*N*)	Abnormal RNFL thickness (*n*/*N*)	Sensitivity (%)	Specificity (%)	PPV (%)	NPV (%)
Tabletop OCT (*N* = 175)						
Average[a]	47/175	106/175	74.5	44.5	33.0	82.6
Superior[b]	47/175	98/175	76.6	51.6	36.7	85.7
Nasal[c]	47/175	97/175	68.1	49.2	33.0	80.8
Inferior[d]	47/175	105/175	70.2	43.8	31.4	80.0
Temporal[e,f]	47/174	93/174	80.9	56.7	40.9	88.9

Abbreviations: NPV, negative predictive value; OCT, optical coherence tomography; PPV, positive predictive value; RNFL, retinal nerve fibre layer.

[a]35/47 eyes (74.5%) with an abnormal visual function had an abnormal average circumpapillary RNFL thickness; 57/128 eyes (44.5%) had a normal visual function and a normal average circumpapillary RNFL thickness.

[b]36/47 eyes (76.6%) with an abnormal visual function had an abnormal superior circumpapillary RNFL thickness; 66/128 eyes (51.6%) had a normal visual function and a normal superior circumpapillary RNFL thickness.

[c]32/47 eyes (68.1%) with an abnormal visual function had an abnormal nasal circumpapillary RNFL thickness; 63/128 eyes (49.2%) had a normal visual function and a normal nasal circumpapillary RNFL thickness.

[d]33/47 eyes (70.2%) with an abnormal visual function had an abnormal inferior circumpapillary RNFL thickness; 56/128 eyes (43.8%) had a normal visual function and a normal inferior circumpapillary RNFL thickness.

[e]Diagnostic accuracy of the temporal retinal nerve fibre layer thickness is missing for one eye.

[f]38/47 eyes (80.9%) with an abnormal visual function had an abnormal temporal circumpapillary RNFL thickness; 72/127 eyes (56.7%) had a normal visual function and a normal temporal circumpapillary RNFL thickness.

These findings may be particularly important for children who are not able to cooperate with traditional VA and/or VF examination at brain tumour diagnosis, and in whom RNFL thickness and GCL-IPL thickness measurements could provide a certain amount of reassurance that the visual function is normal. However, at this stage, these thickness measurements should only serve as a fast diagnostic screening test in the acute stage, which will be followed by a traditional VA and VF examination when the child is feeling more comfortable. Obtaining reliable RNFL thickness and GCL-IPL thickness measurements may be easier than performing a reliable traditional ophthalmological examination in children with a newly diagnosed brain tumour, because OCT imaging is a rapid, non-invasive and objective testing method (Avery, Rajjoub, et al., 2015; Fercher, 2010). In young and non-cooperative children, handheld OCT can be performed under sedation (Avery et al., 2014; Gu et al., 2014). Nevertheless, despite the prospective nature of this study and a standardized ophthalmological screening protocol, OCT imaging was not manageable or was not reliable in 29% of the children, mostly due to logistical reasons or a poor clinical condition of the patient.

Our literature review showed that previous studies only assessed the diagnostic accuracy in children diagnosed with OPG (Nuijts, Imhof, et al., 2021). These studies demonstrated higher overall sensitivity, specificity,

TABLE 4 Characteristics of ganglion cell layer–inner plexiform layer thickness measurements in children with a normal and abnormal visual function.

		Normal visual function			Abnormal visual function		
	Total	Total	OPG	Craniopharyngioma	Total	OPG	Craniopharyngioma
Tabletop OCT	(*N* = 153)	(*N* = 117)	(*N* = 9)	(*N* = 15)	(*N* = 36)	(*N* = 6)	(*N* = 10)
GCL-IPL thickness, median (range), μm							
Average	84 (54–100)	84 (57–100)	76 (61–87)	85 (57–96)	78 (54–94)	62 (54–71)	72 (64–80)
Minimum[a]	81 (45–97)[a]	82 (47–97)	71 (54–85)	83 (47–93)	69.5 (45–91)[a]	51 (45–57)	65 (58–80)
Supero-temporal	83 (58–96)	84 (58–96)	80 (66–86)	86 (68–94)	79.5 (58–92)	62 (58–90)	74.5 (68–81)
Superior	84 (44–104)	84 (54–104)	78 (64–87)	85 (54–98)	78 (44–98)	57 (44–69)	69 (62–77)
Supero-nasal	85 (51–105)	86 (54–102)	74 (54–89)	84 (54–98)	80.5 (51–105)	57 (51–78)	73 (62–83)
Infero-nasal	84 (49–105)	85 (52–105)	71 (55–88)	84 (52–99)	79.5 (49–95)	57 (49–73)	69.5 (59–83)
Inferior	82 (51–100)	83 (51–100)	75 (57–93)	82 (51–94)	76.5 (54–93)	60 (54–69)	69 (60–85)
Infero-temporal	85 (58–101)	86 (58–101)	85 (59–88)	88 (63–96)	85 (59–95)	62 (59–86)	78 (69–89)

Note: Data are presented as median (range).

Abbreviations: GCL-IPL, ganglion cell layer–inner plexiform layer; OCT, optical coherence tomography; OPG, optic pathway glioma.

[a]Measurement of the minimum ganglion cell layer–inner plexiform layer thickness is missing for two eyes.

TABLE 5 Diagnostic accuracy of ganglion cell layer–inner plexiform layer thickness.

Location	Abnormal visual function (*n*/*N*)	Abnormal GCL-IPL thickness (*n*/*N*)	Sensitivity (%)	Specificity (%)	PPV (%)	NPV (%)
Tabletop OCT (*N* = 153)						
Average[a]	36/153	35/153	41.7	82.9	57.1	82.2
Minimum[b,c]	35/152	65/152	61.8	62.4	32.3	84.9
Supero-temporal[d]	36/153	25/153	38.9	90.6	56.0	82.8
Superior[e]	36/153	34/153	44.4	84.6	47.1	83.2
Supero-nasal[f]	36/153	42/153	52.8	80.3	45.2	84.7
Infero-nasal[g]	36/153	35/153	38.9	82.1	40.0	81.4
Inferior[h]	36/153	40/153	41.7	78.6	37.5	81.4
Infero-temporal[i]	36/153	29/153	38.9	87.2	48.3	82.3

Abbreviations: GCL-IPL, ganglion cell layer–inner plexiform layer; NPV, negative predictive value; OCT, optical coherence tomography; PPV, positive predictive value.

[a]15/36 eyes (41.7%) with an abnormal visual function had an abnormal average macular GCL-IPL thickness; 97/117 eyes (82.9%) had a normal visual function and a normal average macular GCL-IPL thickness.

[b]Diagnostic accuracy of the minimum ganglion cell layer–inner plexiform layer thickness is missing for two eyes.

[c]21/34 eyes (61.8%) with an abnormal visual function had an abnormal minimum macular GCL-IPL thickness; 73/117 eyes (62.4%) had a normal visual function and a normal minimum macular GCL-IPL thickness.

[d]14/36 eyes (38.9%) with an abnormal visual function had an abnormal supero-temporal macular GCL-IPL thickness; 106/117 eyes (90.6%) had a normal visual function and a normal supero-temporal macular GCL-IPL thickness.

[e]16/36 eyes (44.4%) with an abnormal visual function had an abnormal superior macular GCL-IPL thickness; 99/117 eyes (84.6%) had a normal visual function and a normal superior macular GCL-IPL thickness.

[f]19/36 eyes (52.8%) with an abnormal visual function had an abnormal supero-nasal macular GCL-IPL thickness; 94/117 eyes (80.3%) had a normal visual function and a normal supero-nasal macular GCL-IPL thickness.

[g]14/36 eyes (38.9%) with an abnormal visual function had an abnormal infero-nasal macular GCL-IPL thickness; 96/117 eyes (82.1%) had a normal visual function and a normal infero-nasal macular GCL-IPL thickness.

[h]15/36 eyes (41.7%) with an abnormal visual function had an abnormal inferior macular GCL-IPL thickness; 92/117 eyes (78.6%) had a normal visual function and a normal inferior macular GCL-IPL thickness.

[i]14/36 eyes (38.9%) with an abnormal visual function had an abnormal infero-temporal macular GCL-IPL thickness; 102/117 eyes (87.2%) had a normal visual function and a normal infero-temporal macular GCL-IPL thickness.

PPVs and NPVs for average RNFL thickness (Avery et al., 2014; Avery, Cnaan, et al., 2015; Fard et al., 2013; Gu et al., 2014; Parrozzani et al., 2018) and average GCL-IPL (Gu et al., 2014) thickness measurements as compared to our subgroup analysis. Possible explanations for these differences could be the larger and homogeneous study groups in previous studies (Avery et al., 2014, Avery, Cnaan, et al., 2015, Fard et al., 2013, Gu et al., 2014, Parrozzani et al., 2018), the lower prevalence of patients with OPG and an abnormal visual function (Avery et al., 2014; Avery, Cnaan, et al., 2015; Fard et al., 2013; Gu et al., 2014; Parrozzani et al., 2018), and the use of different criteria to determine an abnormal RNFL thickness and GCL-IPL thickness (e.g. abnormal criteria were based on the lower fifth and lower first percentile of the normal vision in the OPG group (Avery et al., 2014, Gu et al., 2014)) compared to our study in which we used age-based 95% CI cut-off levels of healthy children. Other studies investigated RNFL thickness measurements in children with craniopharyngioma and reported RNFL

thinning in children with vision loss (Bialer et al., 2013; Mediero et al., 2015); however, these studies did not specifically assess the diagnostic accuracy.

This study also demonstrates that the continuous GCL-IPL thickness (in microns) was greater in children with a normal visual function compared to children with an abnormal visual function, both in the total group of children and in the subgroups of children with an OPG and craniopharyngioma. Although comparing GCL-IPL thickness measurements between groups was not the primary objective of our study, these numbers provide insight into the absolute differences of GCL-IPL thickness seen in daily practice and the potential of GCL-IPL thickness measurements to differentiate between children with a normal visual function and abnormal visual function. A previous study in children with OPGs showed similar results with significantly smaller GCL-IPL thickness in children with an abnormal visual function (Gu et al., 2014). In contrast, the continuous RNFL thickness measurements (in microns) were greater in children with an abnormal visual function when compared to children with a normal visual function, except for the subgroup of children with OPG where the opposite was true. A possible explanation may be that the RNFL thickness was relatively more affected by the presence of papilledema compared to the GCL-IPL thickness (Gu et al., 2014). Papilledema is a common finding in children with a newly diagnosed brain tumour and can contribute to an abnormal visual function and elevated RNFL thickness (Ahuja et al., 2015; Liu et al., 2019; Nuijts, Stegeman, et al., 2021; OCT Sub-Study Committee for NORDIC Idiopathic Intracranial Hypertension Study Group et al., 2014; Sibony et al., 2021). Contrary, in children with an OPG, an abnormal visual function is commonly described as associated with optic disc pallor and subsequent RNFL thinning (Avery et al., 2011; Gu et al., 2014; Zahavi et al., 2018).

A number of important limitations should be acknowledged when interpreting the data from our study. Although the aim of the study was to assess the diagnostic accuracy of RNFL thickness and GCL-IPL thickness in children with all types of brain tumours, this heterogeneity of tumour subtypes, tumour locations and the various ophthalmological findings may affect the interpretation of the study results. For example, in children with a brain tumour and severe papilledema, RNFL thickness measurements were often unreliable due to segmentation errors. We assessed the diagnostic accuracy of RNFL thickness and GCL-IPL thickness measurements in brain tumour subgroups, which are frequently associated with an abnormal visual function (i.e. OPGs and craniopharyngiomas). However, these subgroups were relatively small, limiting drawing solid conclusions about the diagnostic accuracy. Next, we only included children who were able to complete standard ophthalmological examination (i.e. VA or VF examination). Although children who are unable to complete standard ophthalmological examination may benefit the most from OCT imaging, this inclusion criterion was necessary for the study to estimate the diagnostic accuracy of the RNFL thickness and GCL-IPL thickness against the outcomes of ophthalmological examination used in daily practice. Also, we had to accept three different OCT devices in the current study, because not all participating study sites had access to the same OCT device. Each OCT device has its own resolution and computer software algorithm to segment the images and measure the RNFL thickness and GCL-IPL thickness. This could potentially lead to differences in continuous RNFL thickness and GCL-IPL thickness measurements between devices (Pierro et al., 2012). In order to minimalize this device-specific effect, we considered RNFL thickness and GCL-thickness measurements abnormal when they fall outside the age-based 95% CI for the particular OCT device. Regrettably, the GCL-IPL thickness could not be measured with the software of the tabletop Spectralis SD-OCT (Heidelberg Engineering GmbH) and the handheld OCT (Bioptigen), although these devices are used in the minority of the study patients (8.7%). Also, the handheld OCT device was not available in all participating study sites, resulting in a small group of young children (4.1%) without RNFL thickness and GCL-IPL thickness measurements at brain tumour diagnosis. This could have led to an underrepresentation of this particular age group and associated tumour types, such as OPGs. Moreover, age-based cut-off values for abnormal RNFL thickness measurements were lacking for the handheld OCT device (Bioptigen), making it impossible to evaluate the diagnostic accuracy in patients scanned with this device and representing the limitations of handheld OCT in daily practice. Lastly, there is variability in the timing of ophthalmological examination and OCT imaging (i.e. pre- and post-operatively), which could have introduced bias by influencing the RNFL thickness and GCL-IPL thickness measurements. This variability in timing was unavoidable due to a poor clinical condition of some children pre-operatively.

At this moment, we do not recommend using RNFL thickness and GCL-IPL thickness measurements to influence clinical care decision-making in children with a newly diagnosed brain tumour, nor should these measurements replace a thorough ophthalmological examination by a paediatric neuro-ophthalmologist. The main reasons for this recommendation are limitations in retinal layer analyses, the lack of a normality database for children in OCT software and the relatively small subgroup analyses in this study. However, as mentioned before, the relatively high NPVs for the average circumpapillary RNFL thickness and average macular GCL-IPL thickness signify that children with normal thickness measurements at brain tumour diagnosis have a relative high certainty of a normal visual function and as such may be helpful in children who are not cooperative with traditional VA and/or VF examination. The longitudinal data of the CCISS study will be analysed after the completion of the 2 year follow-up. These data will provide more insight into the structure–function relationship between RNFL thickness and GCL-IPL thickness and the visual function and may clarify the potential role of OCT imaging in the ophthalmological evaluation of children with a brain tumour.

In conclusion, our study demonstrates that circumpapillary average RNFL thickness measurements have a relatively moderate sensitivity and low to moderate specificity in discriminating an abnormal visual function in

children with a newly diagnosed brain tumour. Macular average GCL-IPL thickness measurements have a relatively low to moderate sensitivity and high specificity in the detection of an abnormal visual function in the same patient group. The amount of data on retinal OCT in children with a brain tumour is currently still too little to apply in clinical decision-making.

FUNDING INFORMATION

This research was funded by Stichting Kinderen Kankervrij (KiKa) (research grant: number 304; allocated to S.I. Imhof and A.Y.N. Schouten – van Meeteren). The funding organization had no role in one of the following: design and conduct of the study; collection, management, analysis and interpretation of the data; preparation, review or approval of the manuscript; and decision to submit the manuscript for publication.

DATA AVAILABILITY STATEMENT

The data that support the findings of this study are available from the corresponding author upon reasonable request.

ORCID

Myrthe A. Nuijts https://orcid.org/0000-0002-6362-0122
Carlien A. M. Bennebroek https://orcid.org/0000-0002-4733-2120

REFERENCES

Ahuja, S., Anand, D., Dutta, T.K., Roopesh Kumar, V.R. & Kar, S.S. (2015) Retinal nerve fiber layer thickness analysis in cases of papilledema using optical coherence tomography – a case control study. *Clinical Neurology and Neurosurgery*, 136, 95–99.

Armstrong, G.T. (2010) Long-term survivors of childhood central nervous system malignancies: the experience of the childhood cancer survivor study. *European Journal of Paediatric Neurology*, 14, 298–303.

Armstrong, G.T., Conklin, H.M., Huang, S., Srivastava, D., Sanford, R., Ellison, D.W. et al. (2011) Survival and long-term health and cognitive outcomes after low-grade glioma. *Neuro Oncology*, 13, 223–234.

Avery, R.A., Bouffet, E., Packer, R.J. & Reginald, A. (2013) Feasibility and comparison of visual acuity testing methods in children with neurofibromatosis type 1 and/or optic pathway gliomas. *Investigative Ophthalmology and Visual Science*, 54, 1034–1038.

Avery, R.A., Cnaan, A., Schuman, J.S., Trimboli-Heidler, C., Chen, C.-L., Pakcer, R.J. et al. (2015) Longitudinal change of Circumpapillary retinal nerve fiber layer thickness in children with optic pathway gliomas. *American Journal of Ophthalmology*, 160, 944–952.

Avery, R.A., Hwang, E.I., Ishikawa, H., Acosta, M.T., Hutcheson, K.A., Santos, D. et al. (2014) Handheld optical coherence tomography during sedation in young children with optic pathway gliomas. *JAMA Ophthalmology*, 132, 265–271.

Avery, R.A., Liu, G.T., Fisher, M.J., Quin, G.E., Belasco, J.B., Phillips, P.C. et al. (2011) Retinal nerve fiber layer thickness in children with optic pathway gliomas. *American Journal of Ophthalmology*, 151, 542–549.e2.

Avery, R.A., Rajjoub, R.D., Trimboli-Heidler, C. & Waldman, A.T. (2015) Applications of optical coherence tomography in pediatric clinical neuroscience. *Neuropediatrics*, 46, 88–97.

Barrio-Barrio, J., Noval, S., Galdõs, M., Ruiz-Canela, M., Bonet, E., Capote, M. et al. (2013) Multicenter Spanish study of spectral-domain optical coherence tomography in normal children. *Acta Ophthalmologica*, 91, 56–63.

Bialer, O.Y., Goldenberg-Cohen, N., Toledano, H., Snir, M. & Michowiz, S. (2013) Retinal NFL thinning on OCT correlates with visual field loss in pediatric craniopharyngioma. *Canadian Journal of Ophthalmology*, 48, 494–499.

Biousse, V. & Newman, N. (2015) *Optic neuropathies*, 2nd edition. New York: Neuro-Ophthalmology Illustrated.

Bossuyt, P.M., Reitsma, J.B., Bruns, D.E., Gatsonis, C.A., Glasziou, P.P., Irwig, L.M. et al. (2003) Towards complete and accurate reporting of studies of diagnostic accuracy: the STARD initiative. *Annals of Internal Medicine*, 138, 40–44.

Donahue, S.P. & Porter, A. (2001) SITA visual field testing in children. *Journal of AAPOS*, 5, 114–117.

Fard, M.A., Fakhree, S. & Eshraghi, B. (2013) Correlation of optical coherence tomography parameters with clinical and radiological progression in patients with symptomatic optic pathway gliomas. *Graefe's Archive for Clinical and Experimental Ophthalmology*, 251, 2429–2436.

Fercher, A.F. (2010) Optical coherence tomography—development, prinicples, applications. *Zeitschrift für Medizinische Physik*, 20, 251–276.

Greve, E.L., Dannheim, F. & Bakker, D. (1982) The Peritest, a new automatic and semi-automatic perimeter. *International Ophthalmology*, 5, 201–214.

Gu, S., Glaug, N., Cnaan, A., Packer, R.J. & Avery, R.A. (2014) Ganglion cell layer-inner plexiform layer thickness and vision loss in young children with optic pathway gliomas. *Investigative Ophthalmology & Visual Science*, 55, 1402–1408.

Koenraads, Y., Braun, K.P.J., Van Der Linden, D.C.P., Imhof, S.M. & Porro, G.L. (2015) Perimetry in young and neurologically impaired children: the behavioral visual field (BEFIE) screening test revisited. *JAMA Ophthalmology*, 133, 319–325.

Liu, Y., Abongwa, C., Ashwal, S., Deming, D.D. & Winter, T.W. (2019) Referral for ophthalmology evaluation and visual sequelae in children with primary brain tumors. *JAMA Network Open*, 2, e198273.

Louis, D.N., Perry, A., Reifenberger, G., von Deimling, A., Figarella-Branger, D., Cavenee, W.K. et al. (2016) The 2016 World Health Organization classification of tumors of the central nervous system: a summary. *Acta Neuropathologica*, 131, 803–820.

Maldonado, R.S., Izatt, J.A., Sarin, N., Wallace, D.K., Freedman, S., Cotten, C.M. et al. (2010) Optimizing hand-held spectral domain optical coherence tomography imaging for neonates, infants, and children. *Investigative Ophthalmology and Visual Science*, 51, 2678–2685.

Mediero, S., Noval, S., Bravo-Ljubetic, L., Contreras, I. & Carceller, F. (2015) Visual outcomes, visual fields, and optical coherence tomography in paediatric craniopharyngioma. *Neuro-Ophthalmology*, 39, 132–139.

Nuijts, M.A., Degeling, M.H., Stegeman, I., Schouten-van Meeteren, A.Y.N. & Imhof, S.M. (2019) Visual impairment in children with a brain tumor: a prospective nationwide multicenter study using standard visual testing and optical coherence tomography (CCISS study). *BMC Ophthalmology*, 19, 220.

Nuijts, M.A., Imhof, S.M., Veldhuis, N., Dekkers, C.C., Schouten – van Meeteren, A.Y.N. & Stegeman, I. (2021) The diagnostic accuracy and prognostic value of OCT for the evaluation of the visual function in children with a brain tumour: a systematic review. *PLoS One*, 16, e0261631.

Nuijts, M.A., Stegeman, I., Porro, G.L. et al. (2021) Ophthalmological evaluation in children presenting with a primary brain tumor. *Journal of Neuro-Ophthalmology*, 42, 1–10.

OCT Sub-Study Committee for NORDIC Idiopathic Intracranial Hypertension Study Group, Auinger, P., Durbin, M., Feldon, S., Garvin, M., Kardon, R. et al. (2014) Baseline OCT measurements in the idiopathic intracranial hypertension treatment trial, part I: quality control, comparisons, and variability. *Investigative Ophthalmology and Visual Science*, 55, 8180–8188.

Parrozzani, R., Miglionico, G., Leonardi, F., Pulze, S., Trevisson, E., Clementi, M. et al. (2018) Correlation of peripapillary retinal nerve fibre layer thickness with visual acuity in paediatric patients affected by optic pathway glioma. *Acta Ophthalmologica*, 96, e1004–e1009.

Pérez-García, D., Ibañez-Alperte, J., Remón, L., Cristóbal, J., Sanchez-Cano, A. & Pinilla, I. (2015) Study of spectral-domain optical coherence tomography in children: Normal values and influence of age, sex, and refractive status. *European Journal of Ophthalmology*, 26, 135–141.

Pierro, L., Gagliardi, M., Iuliano, L., Ambrosi, A. & Bandello, F. (2012) Retinal nerve fiber layer thickness reproducibility using seven different OCT instruments. *Investigative Ophthalmology and Visual Science*, 53, 5912–5920.

Pillai, S., Metrie, M., Dunham, C., Sargent, M., Hukin, J. & Steinbok, P. (2012) Intracranial tumors in infants: long-term functional outcome, survival, and its predictors. *Child's Nervous System*, 28, 547–555.

Quinn, G.E., Fea, A.M. & Minguini, N. (1991) Visual fields in 4- to 10-year-old children using Goldmann and double-arc perimeters. *Journal of Pediatric Ophthalmology and Strabismus*, 28, 314–319.

Saha, A., Salley, C.G., Saigal, P., Rolnitzky, L., Goldberg, J., Scott, S. et al. (2014) Late effects in survivors of childhood CNS tumors treated on head start I and II protocols. *Pediatric Blood & Cancer*, 61, 1644–1672.

Shah, S.D., Haq, A., Toufeeq, S., Tu, Z., Edawaji, B., Abbott, J. et al. (2020) Reliability and recommended settings for pediatric circumpapillary retinal nerve fiber layer imaging using hand-held optical coherence tomography. *Translational Vision Science & Technology*, 9, 1–10.

Sibony, P.A., Kupersmith, M.J. & Kardon, R.H. (2021) Optical coherence tomography neuro-toolbox for the diagnosis and Management of Papilledema, optic disc edema, and Pseudopapilledema. *Journal of Neuro-Ophthalmology*, 41, 77–92.

Taylor, T., Jaspan, T., Milano, G., Gregson, R., Parker, T., Ritzmann, T. et al. (2008) Radiological classification of optic pathway gliomas: experience of a modified functional classification system. *The British Journal of Radiology*, 81, 761–766.

Traunwieser, T., Kandels, D., Pauls, F., Pietsch, T., Warmuth-Metz, M., Bison, B. et al. (2020) Long-term cognitive deficits in pediatric low-grade glioma (LGG) survivors reflect pretreatment conditions—report from the German LGG studies. *Neuro-Oncology Advances*, 2, 1–18.

Vinchon, M., Baroncini, M., Leblond, P. & Delestret, I. (2011) Morbidity and tumor-related mortality among adult survivors of pediatric brain tumors: a review. *Child's Nervous System*, 27, 697–704.

Zahavi, A., Toledano, H., Cohen, R., Sella, S., Luckman, J., Michowiz, S. et al. (2018) Use of optical coherence tomography to detect retinal nerve fiber loss in children with optic pathway glioma. *Frontiers in Neurology*, 9, 1102.

SUPPORTING INFORMATION

Additional supporting information can be found online in the Supporting Information section at the end of this article.

How to cite this article: Nuijts, M.A., Stegeman, I., Porro, G.L., Bennebroek, C.A.M., van Seeters, T., Proudlock, F.A. et al. (2023) Diagnostic accuracy of retinal optical coherence tomography in children with a newly diagnosed brain tumour. *Acta Ophthalmologica*, 101, 658–669. Available from: https://doi.org/10.1111/aos.15650